DOI 10.4430/bgo00363

A new method for paleostress study on 3D seismic interpretation data, revealing the tectonic evolution in western Zagros, southern Iran

S. Pourbeyranvand[1], M. Gholami Dargahi[2] and I. Abdolahiefard[3]

[1] *International Institute of Seismology and Earthquake Engineering, Tehran, Iran*
[2] *Kharazmi University, Faculty of Earth Sciences, Tehran, Iran*
[3] *National Iranian Oil Company, Exploration Directorate, Tehran, Iran*

(Received: 21 September 2020; accepted: 7 June 2021; published online: 3 December 2021)

ABSTRACT The stress field and its spatial and temporal changes are critical in various branches of geosciences such as geotechnics, petroleum geology, and geomechanical studies of hydrocarbon-bearing reservoirs. It is also crucial in understanding the geodynamics of the area. This investigation also aims to infer the tectonic evolution of the area, which is important for hydrocarbon production. In this study, a new method for determining the slip direction from 3D seismic interpretation data is used for paleostress studies in one of the hydrocarbon fields in southern Iran. The method is implemented for different horizons with different geological ages employing a non-linear stress tensor inversion scheme. The stress direction remains constant for a long time, starting from the Cretaceous based on the horizon's geological ages. Also, the present state of the stress field is calculated from the focal mechanism of earthquakes obtained from international research centres by the same method. This study showed rotation in the direction of maximum horizontal stress over time. The maximum horizontal stress direction of NW-SE in the Cretaceous becomes NE-SW in the present day. Due to the lack of data, it is not possible to conclude whether this rotation is clockwise or counterclockwise, urging more detailed studies**.**

Key words: stress field, inversion, 3D seismic, earthquake, focal mechanism, slip direction.

1. Introduction

In structural geology studies, dynamic analysis, which means determining the direction of effective stresses in the formation of tectonic structures, plays a vital role. Various methods have been proposed for this purpose, including tectonic, geophysical, and instrumental techniques. The tectonic methods are used to determine the direction of stress, including the use of brittle structures (faults) that record the applied stresses (Abbasi and Farbod, 2004). When the faulting occurs, blocks on both sides of the faults move relative to each other in the direction of maximum shear stress due to the force applied to them. Qualitative and quantitative analysis of these brittle structures provides a reliable solution for understanding the distribution and evolution of stress fields from tectonic events. But sometimes, faults may not be exposed at the surface and as a result, the fault slip data may not be available through outcrops. In such cases, the use of interpreted 3D seismic interpretation data can be helpful in paleostress studies. This approach was first proposed by Gartrell and Lisk (2005) and later developed by Lohr *et al.* (2008) and Van Gent *et al.* (2009).

According to Gartrell and Lisk's studies (2005), it is possible to estimate the orientations and magnitudes of paleostresses from seismic data by analysing fault-slip data obtained by using 3D restoration techniques. The results gathered in the case studies are consistent with regional observations. Of course, there are several sources of error regarding the quality of available data, including resolution of the seismic data, the footprint of seismic interpretation, restoration techniques, and inversion methods. Van Gent *et al.* (2009) introduced a new method for reconstructing paleostresses at subsurface layers where fault slip measurements are impossible with traditional methods based on fault outcrops. 3D seismic data and structural restoration were employed to determine fault surfaces and slip vectors. These data were used as input for the paleostress reconstruction algorithm and a stepwise method was selected to remove younger deformations to obtain slip vectors related to older deformation events. Also, the presented results were consistent with the interpretation of paleostress in the study area (Van Gent *et al.*, 2009). In the present study, the non-linear inversion method is used for dynamic analysis of the fault slip information (strike Φ, dip δ, rake λ) resulting from 3D seismic data and the focal mechanism of the earthquakes. The purpose of this study is to review the results of paleostress studies in the sedimentary cover and compare it with the current state of stress and determine the tectonic evolution of the south-western Zagros through these investigations.

2. Data

The data used in this study are divided into two separate classifications, including a 3D seismic cube (section 2.1) and earthquake focal mechanisms (section 2.2). Several horizons and one fault plane have been defined and interpreted on the 3D seismic cube. This data set is, then, used for implementing the new method of slip direction estimation. The paleostress field is estimated based on the obtained slip directions for different horizons or various geological times, respectively. The present state of the stress is, then, determined using the inversion of the earthquake focal mechanism data (section 3).

2.1. 3D seismic data

The interpreted 3D cube, with an area of 600 km^2, covers a hydrocarbon field in south-western Iran. The length of the fault zone within the 3D cube is measured ~35 km and its estimated depth is more than 10 km. This is a deep-rooted N-S trending strike-slip fault zone with a very steep or near-vertical plane. The interpreted horizons at both sides of the fault plane have been carefully intersected to the fault to enable the displacement across the fault zone. The interpreted horizons intersected by the fault are shown in Fig. 1, as well as the set of pairs of separation points discussed in detail

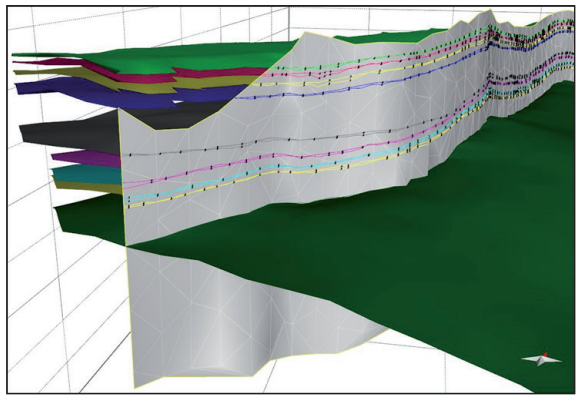

Fig. 1 - The intersection of some interpreted horizons with the main fault of the region and Allan lines resulting from the intersection and a pair of separation points.

below. The Allan lines are the intersection of the horizons with the fault plane. The horizons and their geological ages are displayed in Fig. 2 as the stratigraphy column of the study area. The depth map of the top Fahliyan Formation (Berriasian-Valanginian) in relation to the fault zone is shown in Fig. 3 (Pourbeyranvand, 2012; Tayeb Hosseini *et al.*, 2017).

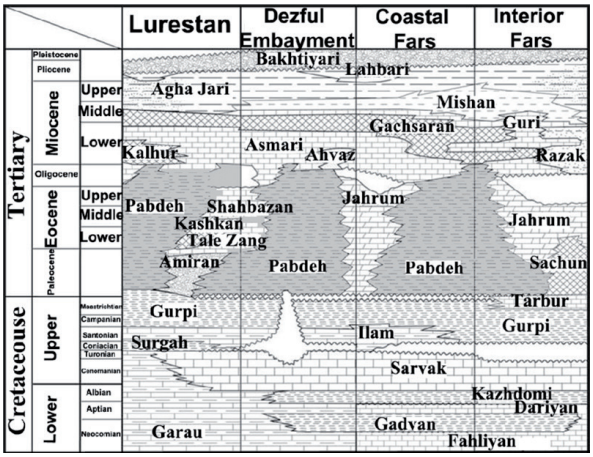

Fig. 2 - Stratigraphic column of the Zagros area in geological times under study (Sepehr and Cosgrove, 2004).

According to Fig. 2, there is a hiatus between the Sarvak Formation (Cenomanian-Turonian) and the overlying strata. This surface is defined with an erosional unconformity surface according to the well and seismic data. This discontinuity and thickness variations of the Sarvak Formation are due to the uplifting in mid-Turonian time due to compression applied by obduction of Oman Ophiolites (Searle, 2019). Linear changes in the basin's topography may reflect early displacements at the basement level along the fault zone. According to the previous studies, the maximum activity of the faults occurred simultaneously with the deposition of Bangestan Group formations (Sarvak and Ilam); thus, it caused thinning and erosion of these two formations during the Late Cretaceous. Also, both the Upper Cretaceous Gurpi and Tertiary Pabdeh and Asmari formations were thinned along the fault zone, representing its reactivation during deposition of these formations. Even thickness of the post-Asmari layers changes across the fault zone, which suggests that this fault zone was active in Neogene and its activity somewhat has been intensified by the collisional forces of the Zagros Orogeny (Tayeb Hosseini *et al.*, 2017).

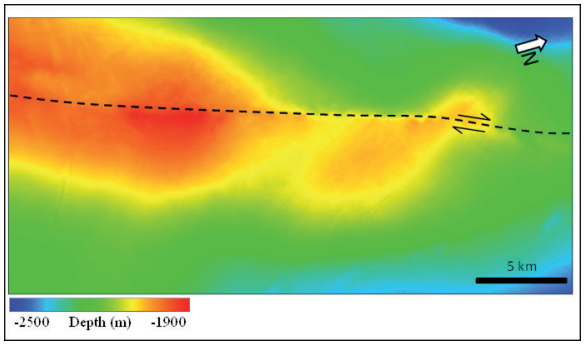

Fig. 3 - Depth map of the top Fahliyan Formation (Pourbeyranvand, 2012).

2.2. Earthquakes focal mechanisms in the western Zagros

Focal mechanisms are valuable sources of information about the relative directions and magnitudes of stress in the crust. The use of focal mechanisms to connect earthquakes with faults, especially in areas with tectonic complexity, is always instructive. Since surface rupture with seismic activity is rare in the Zagros, most of the information about active faults in this region is obtained from earthquakes (Talebian and Jackson, 2004). In the present study, an attempt has been made to estimate the crustal stress in the study area in the western Zagros using the inversion of the focal mechanisms of earthquakes. The stress tensor cannot be obtained with certainty using a single earthquake focal mechanism (McKenzie, 1969). We know from past experience that a cluster of at least 20 to 30 earthquakes is required to obtain optimal results from the inversion of focal mechanisms (Lund and Bödvarsson, 2002). In this regard, an attempt has been made to use all available valid focal mechanisms available for earthquakes in this active seismic zone. The local and seismic data used in this study include data solved by the CMT method and focal mechanisms in the U.S. Geological Survey (USGS) database for the study area (Fig. 4).

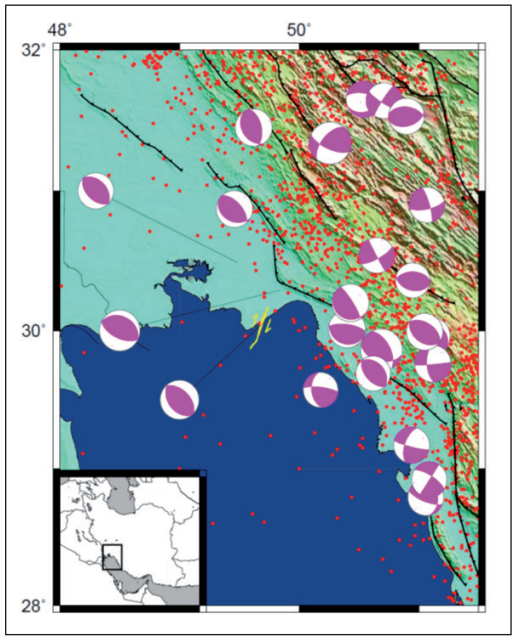

Fig. 4 - The main fault, along with seismicity with a combination of catalogues of the Institute of Seismology and Earthquake Engineering, until 2006 (IIEES, 2006) and the Institute of Geophysics, the University of Tehran, since 2006 (IRSC, 2020), and available focal mechanisms from Global Moment Tensor Project (GCMT, 2020).

3. Methods

Again the method part consists of two different sections. One describes the innovative new approach to paleostress study through slip direction estimation based on 3D seismic interpretation data (section 3.1). The other one deals with the formal stress tensor inversion, which should be applied to both data sets. The first data set uses the outcomes of the first method or paleo-fault-slip data, which should be inverted for obtaining the paleostress filed. The second data set is the earthquake focal mechanism data, which should be inverted for getting the present stress state. The results of the application of the stress inversion on both data sets are, then, compared in the discussion (section 5) to investigate the tectonic evolution of the region.

3.1. New method of fault slip direction estimation

For stress tensor inversion, as mentioned earlier in the introduction and will be discussed in more detail in the next part (section 3.2), fault slip data such as strike Φ, dip δ, and rake λ (maximum shear stress direction) are required as the necessary inputs of the method. Using structural geology modelling software, the 3D surface of the fault was latticed by triangulation. Each triangle forming the fault's surface was considered as a separate fault plane (Fig. 5). Although the fault plane, in general, can be distorted, each triangle is flat. The sizes of the triangles are not the same because of undulations along the fault plane. The lengths of the sides of an optional triangle can vary roughly from several tens of metres up to few hundreds of metres, remembering that the triangles can be chosen regarding the desired predefined criteria so that they do not exceed the spatial resolution or uncertainty of the data. By intersecting these triangular fault planes with the horizons, the Allan lines (Allan diagram) are constructed, which play an important role in determining the slip angle of rake (λ).

Regarding the extraction of fault slip data, the strike (Φ) and dip (δ) of each fault plane (each triangle) were easily obtained exactly from its 3D structural model and directly from the mentioned modelling software. However, calculating the rake (λ) is always the most challenging part of paleostress studies using seismic data. Regarding the rake (λ) extraction, its calculation was performed using the separation pairs provided by the inclined shear algorithm of the mentioned software. Here, the relationship between the slip vector and the separation pairs is discussed, and a formula for the calculation of λ will be addressed. The relation of the rake or slip vector with the pair of separation points is that this pair of hypothetical points, which were part of an integrated horizon and were adjacent to each other, are now separated due to the occurrence of the faulting before the faulting occurred. These points offset from each other on two different sides of the horizon with respect to the intersecting fault plane. The hypothetical line connecting the two points indicates the direction of the fault displacement or the slip direction on the fault plane (Fig. 5). Therefore, the transport vector of the separation pair is the same as the slip vector, and the angle of that vector with the fault strike is the same as the slip angle of rake (λ) (Fig. *6*). An important issue is to find the locations of these two points on the fault plane after the faulting.

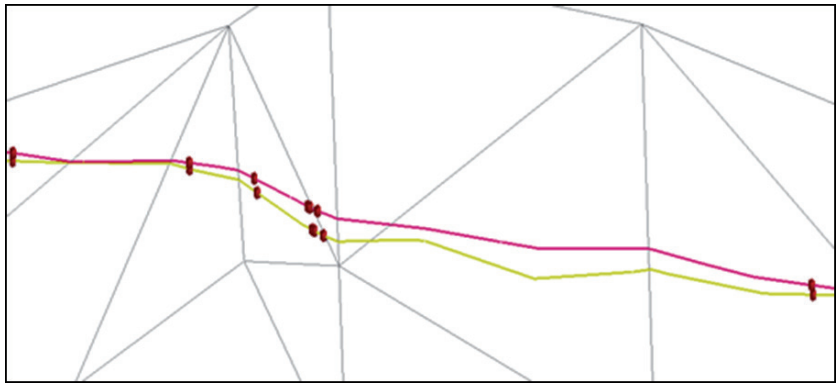

Fig. 5 - Allan lines (red or darker and yellow or lighter) are both attributed to one of the horizons fragmented by the main fault and some separation pairs as examples. The constituent triangles of the fault surface are also plotted in gray (Pourbeyranvand, 2012).

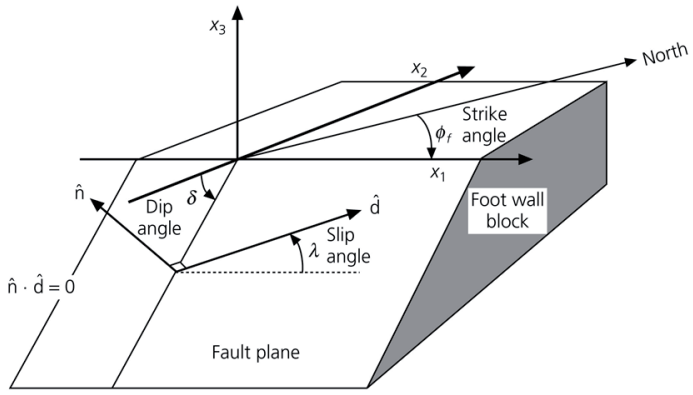

Fig. 6 - The hypothetical vector *d* is the same as the fault displacement vector or the line joining the theoretical separation pairs, and the parameter λ also indicates the rake (Stein and Wysession, 2003).

According to what has been discussed, assuming the separation pairs' coordinates, it is possible to formulate and calculate the slip angle of rake λ (the spatial angle between the vector connecting two separation pairs) and the fault strike vector. First, the vector connecting the separation pairs (displacement vector or slip vector) system is indicated in the Cartesian coordinates:

$$(\Delta X, \Delta Y, \Delta Z) = (X_1 - X_2, Y_1 - Y_2, Z_1 - Z_2) \quad (1)$$

The fault strike can also be written with respect to the north (the rotation is considered clockwise) as follows:

$$(sin\phi, cos\phi, 0) \quad (2)$$

We know that the angle between two arbitrary vectors **a** and **b** is calculated from the following equation:

$$\lambda = cos^{-1} \frac{a \cdot b}{|a| \cdot |b|} \quad (3)$$

Therefore, by substituting vectors (Eqs. 1 and 2) instead of vectors *a* and *b* in Eq. 3, respectively, the slip angle of rake (λ) is finally obtained in the following simplified form:

$$Rake = \pm\lambda = cos^{-1} \frac{\Delta X \cdot sin\phi + \Delta Y \cdot cos\phi}{\sqrt[2]{\Delta X^2 + \Delta Y^2 + \Delta Z^2}} \quad (4)$$

Eq. 4 is based on the coordinates of the *X*, *Y*, and *Z* of the separation pairs, which are among the model's outputs. Negative and positive signs in λ are due to the fact that, by definition, rake values include intervals between -180° to +180°. To explain the extraction of the separation pairs with the inclined shear algorithm, we must first define the shear plane, which is a flat plane, always perpendicular to the horizon plane, with 360° of freedom for its azimuth. By implementing the inclined shear algorithm on the interpreted 3D seismic data, from the intersection of a shear

plane with each pair of Allen lines, two points are obtained, referred to as separation pairs. The reason for attributing a pair of Allen lines to a horizon is that the faulting divides an integrated horizon into two distinct parts on either side of the fault. Since each separate part has a particular interface with the fault plane, two different Allen lines appear on the fault plane. Therefore, in each intersection, only one separation point is extracted from each Allen line for a horizon. A pair of separation points called a 'separation pair' is extracted from the two Allen lines. Of course, the intersections must be applied evenly along the Allen lines. Note that in a single azimuth, since the fault surface can be distorted, the slip angles obtained from across the Allen lines can be different. However, their projections are still parallel to each other and also to the intersecting plane azimuth on the horizon plane (Figs. 7 and 8).

As mentioned earlier about finding the slip angle of the rake (λ), the important thing is to find the precise coordinates of the separation pairs on the fault plane on different sides of the splitted horizon. This problem requires finding the correct azimuth for the intersecting plane so that the selected azimuth is appropriate to the slip angle or rake (λ). Here the situation requires knowledge of the geology of the fault and the mechanism of the faulting. We know from the earthquake focal mechanism and the region's previous structural geology that the faulting mechanism on the fault under investigation is almost pure strike-slip. The 3D seismic interpretation data also supports this conclusion by obtaining nearly 90° dipping hanging wall and footwall, implying pure strike-slip motion on the fault. We need to choose an azimuth for the intersecting plane that exhibits the displacement on the fault plane as much as possible. Therefore, the best angle is determined to be parallel to the fault plane in this case study. Obviously, for other cases, the azimuth of the intersecting plane should be selected carefully, according to the structural geology of the study area.

Heave, throw, and fault displacement data are direct outputs of the used modelling software, which can have different values depending on the azimuth selected for the intersecting plane. Knowing the definitions of the above three quantities and the geometric relations between them, we use the coordinates of the *X*, *Y*, and *Z* of the separation pairs to calculated the values of these three quantities to validate the proposed method. Then, we compare these calculated data with the observed one as it is usual in geophysical modelling. As expected, the results of this comparison indicate high compatibility between heave and throw, so that the two diagrams are precisely the same. Figs. 7 and 8 show the observation data in blue (solid line) and the calculated data in red (dashed line).

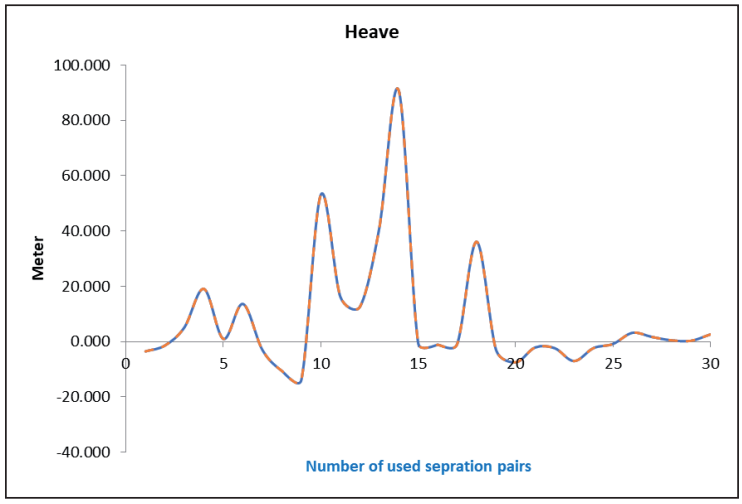

Fig. 7 - The heave in the Kazhdumi Formation belonging to the Cretaceous period. Blue colour (solid line) for observed data. Red (dashed line) for calculated data (explanation in text).

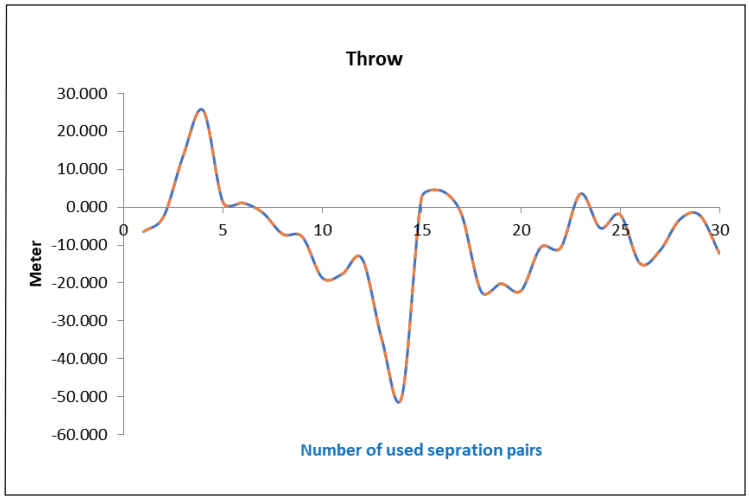

Fig. 8 - The throw in the Kazhdumi Formation belonging to the Cretaceous period. Blue colour (solid line) for observed data. Red (dashed line) for calculated data (explained in the text).

But in the case of fault displacement, there is a discrepancy between the calculated and observed values as expected (Fig. 9). The distortion or non-flatness of the fault plane is the reason for this difference in two ways. Firstly, this causes the Allan lines to be distorted so that, at certain angles, the intersection of the shear plane with the Allan line is more than one point. As we know, the intersection of a smooth plane with a straight line will be only one point, but if the line is distorted, the number of intersections can increase. For solving this problem, that line can be decomposed into several straight lines with the help of the same modelling tool (before intersecting the shear plane with that distorted line), then apply the intersection and, thus, reduce the error as much as possible. Secondly, if the separation pairs belong to two different triangles, then, the calculated value for the fault displacement will always be less than the software's output value unless the two triangles are both connected having the same normal vector. To handle this issue, more accurate calculations can be done on a case-by-case basis with geometric techniques and the amount of error can be minimised or even reduced to zero.

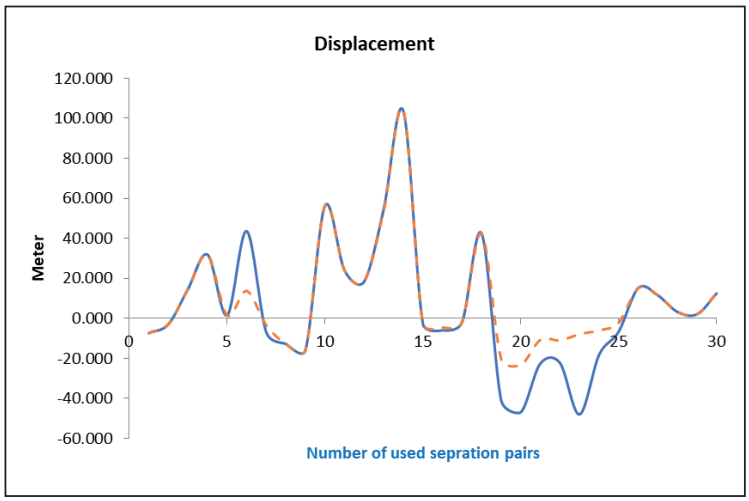

Fig. 9 - Comparison of the slip (fault displacement) in Albian Kazhdumi Formation. The vertical and horizontal axes represent the displacement in metres and points along the Allan lines of a horizon. Blue colour (solid line) is for observational data and red (dashed line) represents computational data (explanation in text).

As it can be seen from the graphs (Figs. 7, 8, and 9), the absolute value of the calculated quantities is always equal to, or less than, the absolute value of the software's output. In other words, the calculated values never exceed the software's output values.

To summarise the above mentioned new method for extraction of fault slip data necessary for paleostress studies, these steps are mentioned assuming a cloud of scattered 3D data point having *X*, *Y* in metres (northing and easting) and *Z* (depth) in kilometres in hand:

- importing the 3D scatter data point in a structural geology modelling computer software and constructing different horizons and the fault plane intersecting the horizons;
- drawing Allan lines or Allan diagrams from the intersection of the fault plane and the horizons. The intersection of the fault plane with each horizon constructs two separate Allan lines;
- obtaining separation pair data from intersecting a vertical plane perpendicular to the fault plane (and also horizontal plane) with the Allan lines;
- reading the azimuth (or strike) and dip of the rectangles on the fault plane surface containing the separation pairs;
- calculating the slip direction or rake using the coordinates of the separation pairs by using the proposed formula;
- stress tensor inversion using the strike, dip, and rake of the obtained fault slip data to get the principle paleostress direction;
- stress tensor inversion of the earthquake focal mechanism data to get the present state of the stress;
- comparing the paleostress direction to the present one to get an insight into the tectonic evolution of the study area.

3.2. Formal stress tensor inversion

There are several linear and non-linear algorithms for stress inversion. Using different methods to study the stress state has the advantage that if the results are similar, then, the findings will have a higher reliability level. On the other hand, according to the previous knowledge about the geology of the study area, it is possible to review both methods' results and introduce a technique that provides a better answer. The advantage of linear methods is that they are more efficient and faster, do not require an initial guess and are easier to obtain. In contrast, non-linear methods require fewer assumptions and give a more realistic answer (Pourbeyranvand, 2012). In the present study, the Lund and Slunga (1999) non-linear inversion method has two approaches: slip angle and instability. In this inversion method, based on the ideas of Gephart and Forsyth (1984), the angle between the directions of shear stress and the direction of slip observed in the fault plane is minimised (Gephart and Forsyth, 1984; Lund and Slunga, 1999). Shear stress on a plate with normal vector $n = (n_1, n_2, n_3)$ is shown as follows (Armijo *et al.*, 1982):

$$\tau = (\sigma_1 - \sigma_3)[Kn_1\,, (K-R)n_2\,, (K-1)n_3] \tag{5}$$

Here, σ_1 and σ_3 are the magnitudes of the maximum and minimum principal stresses, *R* is the stress ratio as $R = (\sigma_1 - \sigma_2)/(\sigma_1 - \sigma_3)$, and $K = n_3^2 + Rn_2^2$.

The angle between the direction of shear stress τ and the direction of the observed slip *s* inside the fault plane is as follows:

$$\alpha = \arccos(\tau \cdot s) \quad (6)$$

The angle α, referred to as the angle of deviation, is what Gephart and Forsyth (1984) refer to as the misfit. This angle is minimised during the inversion (Gephart and Forsyth, 1984; Lund and Slunga, 1999). For each stress tensor, a set of focal mechanisms for all events is examined. Choosing the correct fault plane from two nodal planes in solving the fault plane is one of the main problems of the earthquake focal mechanism stress tensor inversion. Selecting the wrong fault planes will apparently result in incorrect stress tensor.

Here, the inversion algorithm selects the fault planes with two different pre-mentioned slip angle (SA) and instability (IS) methods. In the SA method, the inversion algorithm selects the nodal plane in which the angle between the calculated maximum shear stress direction and the observed slip direction is the smallest. In other words, it chooses the answer with the smallest misfit only from a mathematical point of view. However, this method does not provide a physical insight for the selection of the fault plane. But in the IS method, the inversion algorithm selects the nodal planes, which are more unstable in the current stress field based on Coulomb's Mohr conditions (Lund and Slunga, 1999; Gartrell and Lisk, 2005). Both methods were used for inversion of the data obtained from 3D seismic interpretation and also earthquake focal mechanisms data. Then, the results were compared to ensure the values' preciseness, increasing the reliability of the solutions.

4. Results

Here, the non-linear stress inversion method proposed by Lund and Slunga (1999) is implemented regarding both SA and IS methods. First, the fault slip data from 3D seismic interpretation data is used for paleostress study and, then, the earthquake focal mechanisms are inverted to calculate the present state of the stress. The paleostress inversion results for the horizons intersected by the main fault with an appropriate plane are shown in Fig. 10 by the SA method. Also, the results of the inversion of the earthquake focal mechanisms, revealing the present state of the stress, are shown in Fig. 11 by the SA method. The same inversion results are shown in Figs. 12 and 13 by using the IS method. These results include the direction of the principal stress axis, the confidence limits for σ_1 and σ_3, the histogram of the relative magnitude of the stress $R = (\sigma_1 - \sigma_2)/(\sigma_1 - \sigma_3)$ and the poles to plane Camb contours on the stereonet (Lund and Slunga, 1999). In the SA method, using 3D seismic data, 28 to 36 pairs of separation point data were extracted from four different horizons of various ages that intersected with the fault plane at multiple depths. The results of paleostress inversions are shown on stereonets (Fig. 10).

Also, in the SA method, 17 earthquake focal mechanisms are inverted and the results are displayed on the stereonet (Fig. 11).

Then, the IS method was applied to the data leading to more reliable results according to a more realistic and physically based concept (Figs. 12 and 13).

From all the obtained results, it is clear that while matching both methods' results, the IS method has a comparative advantage over the SA method. As previously mentioned, the confidence limits of the stress axes on the streonets indicate the inversion quality and the IS method is acting better in this regard.

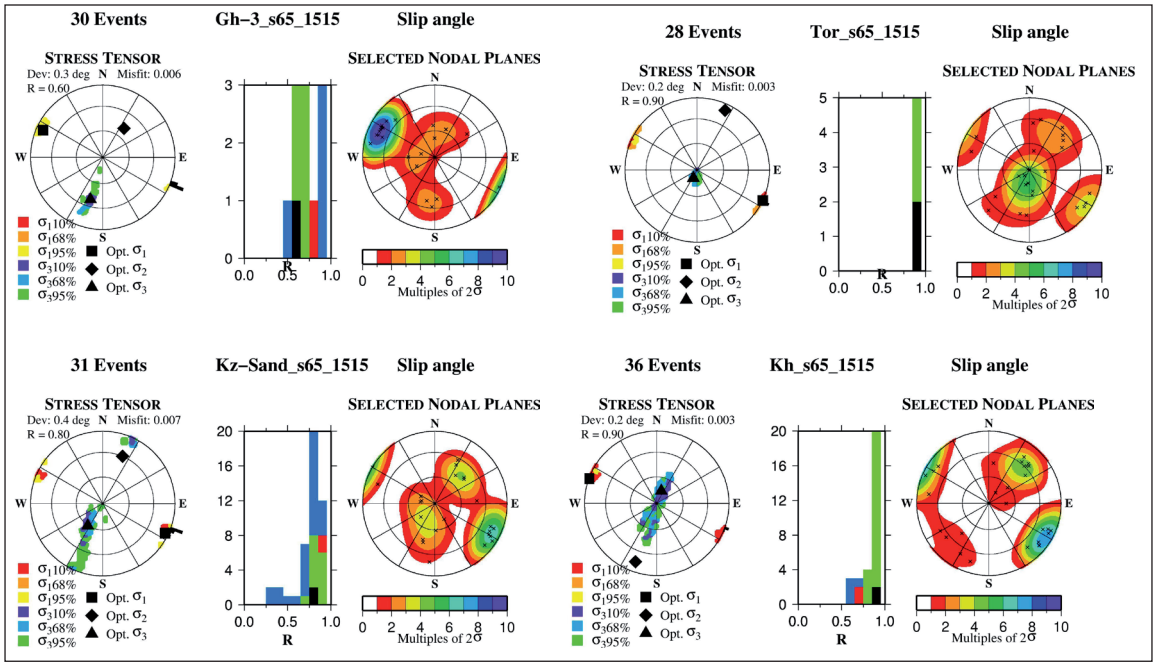

Fig. 10 - The results of Lund and Slunga (1999) paleostress inversion by the SA method on 3D seismic data. To the left are the resulting optimal stress tensors, σ'_1 square, σ'_2 diamond, and σ'_3 triangle; together with the 10, 68, and 95% confidence limits for σ'_1, from red to yellow and σ'_3, from purple to green, both from 10 to 95%. The black histogram on the perimeter shows the 95% confidence level for maximum horizontal stress direction. In the middle are histograms of the 10, 68, and 95% confidence limits for *R* in green, red, and blue, respectively. The black spike is the optimum value. To the right are Kamb contours of the fault plane normals chosen by the inversion. Dariyan (bottom, right), Kazhdumi (bottom, left), Sarvak (top, right) and Asmari (top, left) formations.

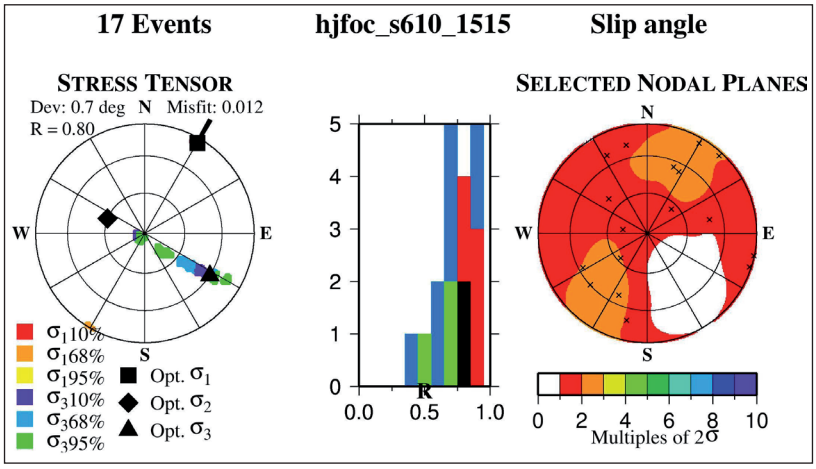

Fig. 11 - The result of stress inversion by the SA method on the earthquake focal mechanism data.

The obtained results are also quantitatively mentioned in Table 1. The maximum horizontal stress direction calculated by both SA and IS methods for all formations intersecting the fault plane and the focal mechanisms of earthquakes are recorded in this table. Here, focal mechanisms represent the present-day stress state, and other titles refer to the formations

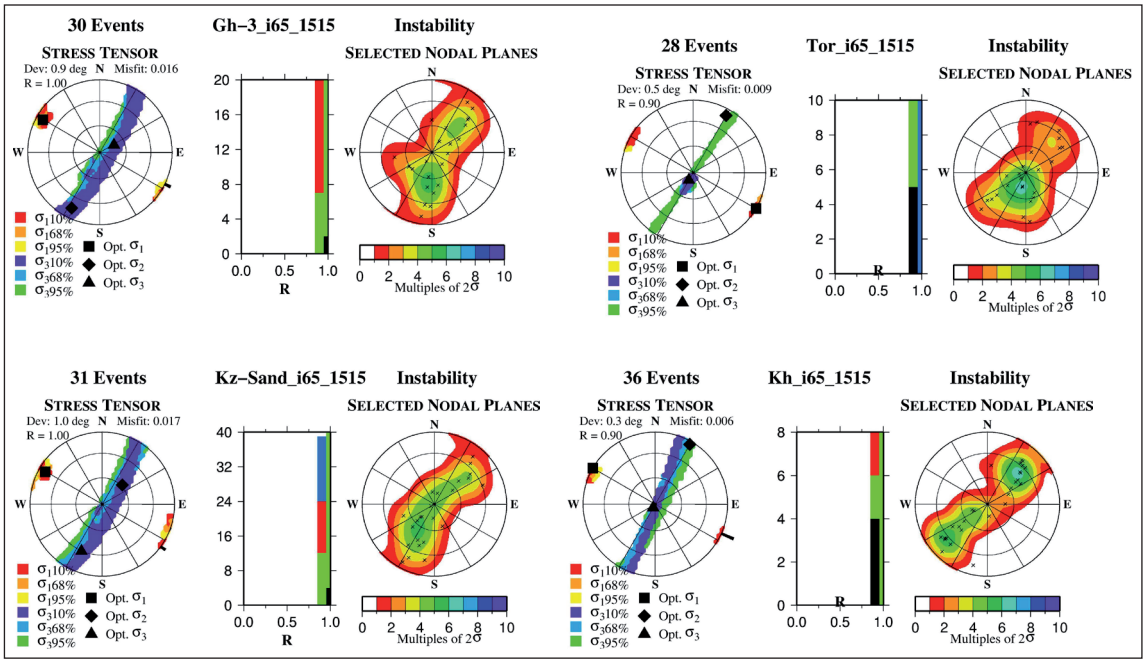

Fig. 12 - The results of Lund and Slunga (1999) paleostress inversion are interpreted by the IS method on 3D seismic data. Dariyan (bottom, right), Kazhdumi (bottom, left), Sarvak (top, right) and Asmari (top, left) formations.

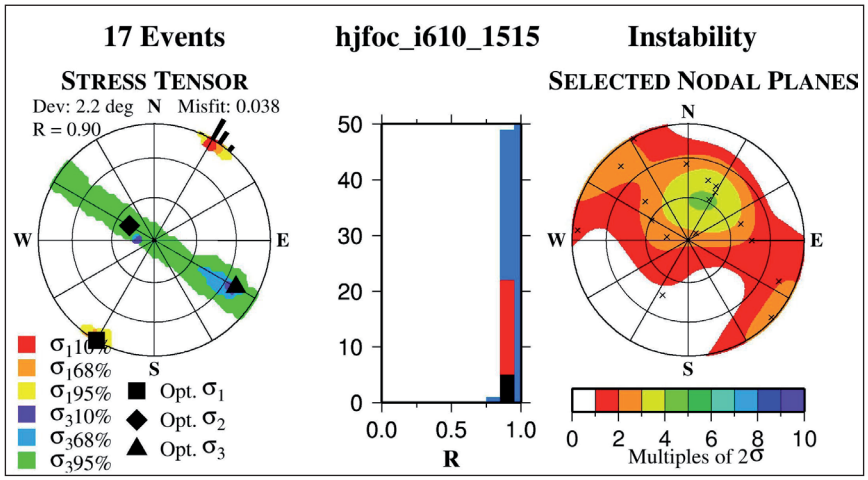

Fig. 13 - The result of stress inversion by the IS method on the earthquake focal mechanism data.

and the paleostress orientation at their specific geological time. Due to the uncertainty in the fault slip data from the seismic interpretation and the earthquake focal parameters, the error in the results can be up to 6° (Keiding *et al.*, 2009; Kumar *et al.*, 2017). The maximum horizontal paleostress has been approximately constant from the Cretaceous to the beginning of the Oligocene period. There are some minor changes in the direction, but the range of variations is small (below 6°), which occurs within the range of the uncertainty and is negligible, therefore.

Table 1 - Quantitative results of inversion of paleostress and present-day stress by SA and IS methods.

No.	Formation	method	SHmax
1	Dariyan	SA	113
		IS	117
2	Kazhdumi	SA	113
		IS	119
3	Sarvak	SA	118
		IS	124
4	Asmari	SA	115
		IS	120
5	Focal mechanism	SA	30
		IS	33

The rake calculation deals with the spatial orientation of the triangular fault plane, which depends on the coordinates of the vertices of the triangles. Therefore, any error in the coordinates of the vertices will cause an error in the calculation of the rake. The accuracy of the seismic data used in this paper, or, in other words, the coordinate error of the vertices, is 25 m. Since the dimensions of the triangles forming the fault are much more than 25 m, the spatial orientation of each triangle does not change much in result of variations in the coordinates of the points. Consequently, the error in the rake will be very small and negligible.

5. Discussion

With respect to the paleostress studies conducted here, the directions of maximum horizontal stress (SHmax) remained constant for a long time on a geological scale from the Early Cretaceous to the Oligocene (middle Tertiary). These directions were obtained in the Cretaceous period from the Khami group's formations, including the Dariyan and Bangestan groups, including Kazhdumi and Sarvak formations. The direction of maximum horizontal stress was also obtained in Oligocene and Early Miocene from the Asmari Formation. All of the above-mentioned principle stresses show the NW-SE direction. Thus, the maximum horizontal stress force during the Cretaceous up to the Oligocene period acts from the Indian subcontinent on the Eurasian tectonic plate.

On the other hand, in the middle Oligocene, the collision between the Arabian and Eurasian plates occurs in the Zagros (Agard *et al.*, 2011; Gholami Zadeh *et al.*, 2017). This collision was associated with a change in the direction of maximum horizontal stress in the study area. Regarding the stress of the present time, as can be seen in the stereonets of Figs. 11 and 13 and Table 1, the direction of maximum horizontal stress direction resulting from the inversion of the focal mechanism of earthquakes shows the NE-SW orientation. This direction is almost

perpendicular to the direction of paleostress under discussion. This fact indicates that rotation has taken place in the direction of principal stresses in the study area. This rotation is under the influence of the collision of Arabian and Iranian plates, which was initiated during the Oligocene and continued later on in the form of the Zagros orogeny. The current state of stress is illustrated in Fig. 14 on the World Stress Map (2020). In addition to the study area, the current state of stress in neighbouring regions, whose data are mainly single focal mechanisms, is plotted.

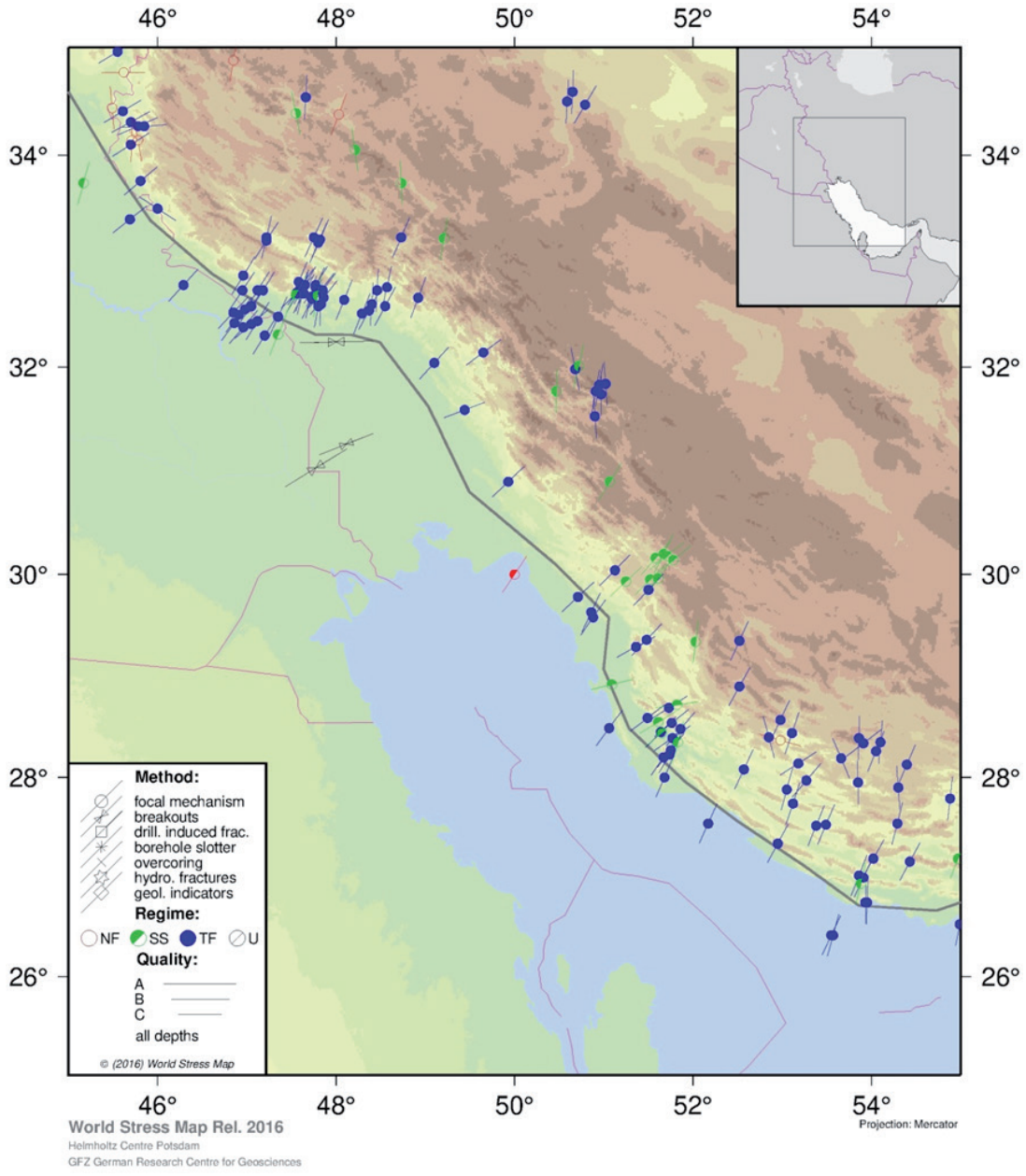

Fig. 14 - The current state of maximum horizontal stress resulting from the inversion of focal mechanisms with a red symbol in the centre of the image, compared to data from the world stress map in the region [obtained through the World Stress Map (2020) project]. Other symbols are described in the map guide.

The paleostress and the present-day stress directions obtained from stress inversions are shown on the stereonets in Fig. 15, to summarise the obtained results and investigate the tectonic evolution of the study area. The stratigraphic and geological time columns are interconnected. Despite the observation of a difference of about 90° in comparing the paleostress and present-day stress directions, there is no gradual trend indicating the direction of rotation occurred between these two states. In other words, since the available data do not show any intersection between the younger horizons and the fault plane, it is not possible to comment on whether the rotation of the stress directions starting from Oligocene up to the present time has occurred clockwise or counterclockwise.

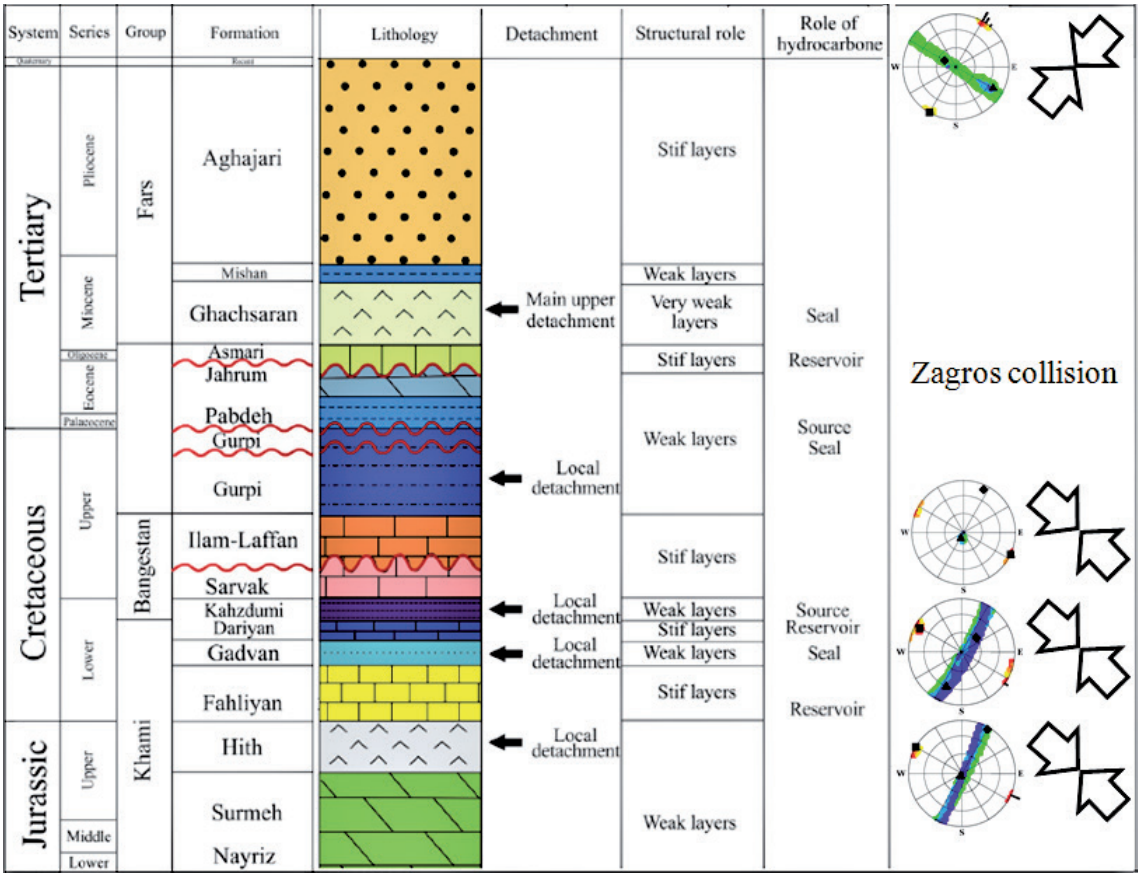

Fig. 15 - Tectonic evolution over time (modified from Kazem Shiroodi *et al.*, 2015). The three stereonet drawn in the lower part of the image, from before the collision and at the same time as the Cretaceous period, represent the direction of maximum horizontal stress in the old testament. The single stereonet at the top of the image also represents the direction of maximum horizontal stress in the present age.

Hydrocarbon reservoirs' existence increases the importance of understanding the tectonic evolution of this area and adjacent regions. The elongation trend of the region's hydrocarbon reservoirs, as shown in Fig. 16, is parallel to the paleostress maximum compression direction. On the other hand, this elongation is perpendicular to the current direction of the maximum stress.

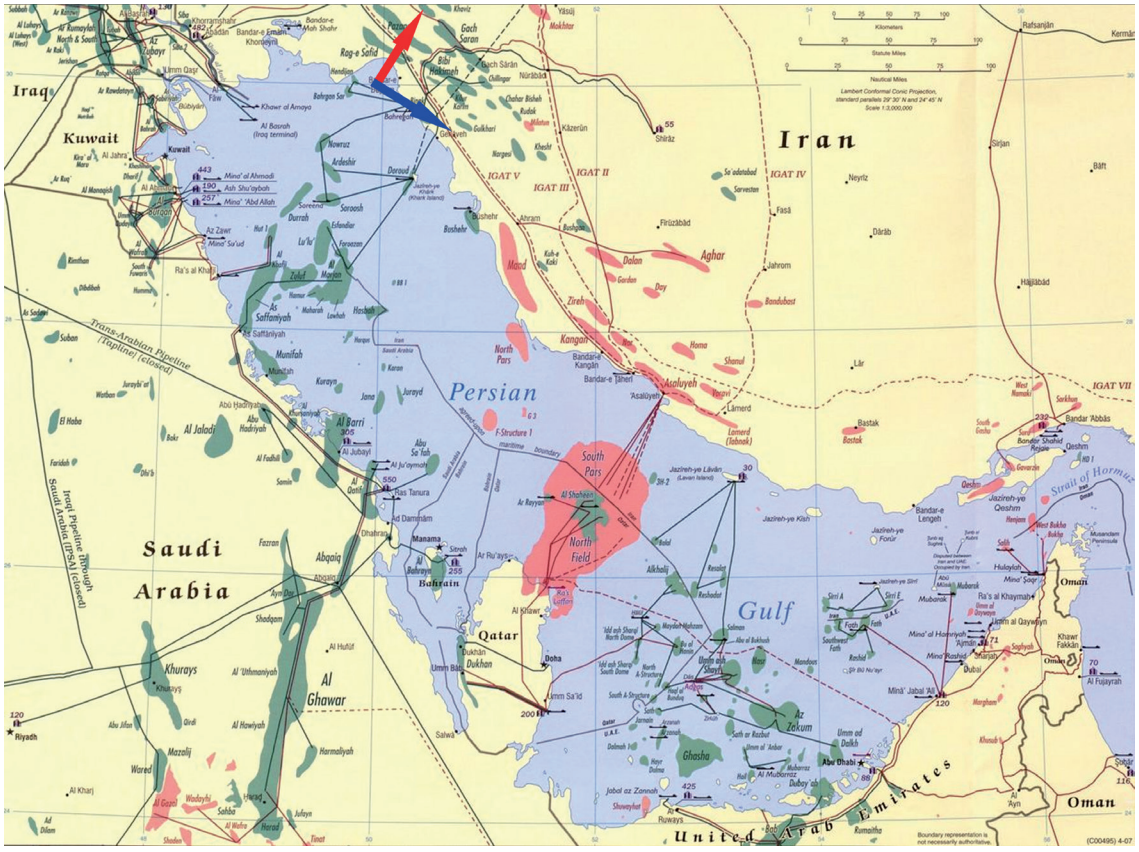

Fig. 16 - Middle east oil and gas reservoirs (modified after the Central Intelligence Agency, 2007). Oil reservoirs are green and gas reservoirs are red. The elongation axis of the reservoirs in the Iranian territory is parallel to obtained paleostress direction and perpendicular to the present maximum compressional stress direction resulting from the Arabian and Eurasian plates' convergence. The present and paleostress maximum horizontal directions are shown on the approximate location of the reservoir by red and blue arrows, respectively.

The deep-seated, possibly basement faults are critically important in the entrapment of hydrocarbon, so it is helpful to know more about such faults in the exploration and development of oil and gas fields (Tayeb Hosseini *et al.*, 2017). Although the geological age of the source or reservoir rocks of these hydrocarbon fields is the same as the age of the horizons studied in the present paleostress study, the age of the deformation, oil trap formation, secondary hydrocarbon migration, and final entrapment of the fluids are related to the time of the collision and afterwards. This is because the direction of these hydrocarbon reservoirs is always parallel to the axis of the folds, anticlines, and synclines, which are themselves the result of the forces applied by the collision of the Arabian plate with Eurasia in the study area.

6. Conclusions

In this study, the paleostress field was estimated at different horizons with various geological ages in one of the hydrocarbon fields in southern Iran, using a new method to determine the fault slip direction from the interpreted 3D seismic data. Based on the present results obtained from non-

linear stress inversion of 3D seismic interpretation data, the direction of maximum horizontal stress remained constant (NW-SE) over a long period of time from the Early Cretaceous to the Oligocene period (Lower Tertiary). This fact indicates that the direction of the maximum horizontal stress in this time interval is under the influence of the convergent force from the Indian subcontinent. However, the results obtained from the focal mechanism of earthquakes, which is consistent with the current regional stress map, confirm that the main stress direction has become NE-SW recently. Thus, a rotation in the direction of maximum horizontal stress direction has occurred in western Zagros so that the current stress is almost perpendicular to the previous paleostress orientation. However, it is not possible to comment on the discussed rotation direction due to the lack of data required. More data and investigations are needed for this purpose.

Acknowledgments. We thank the anonymous reviewers who played a significant role in the improvement of this article. Early versions of this paper were reviewed by A. Javaherian and H. Shomali, resulting in helpful guidance and comments. Special thanks go to B. Lund for providing the stress inversion code STI for this study in addition to training alongside many other helps and supports. The first author appreciates Petex (formerly Midland Valley) company for providing an academic license for using the Move [MOVE Core (Software), 2009] package. He also thanks A. Pourbeyranvand for helping with graphical illustration. Some of the plots are generated using the GMT software (Wessel *et al.*, 2019).

REFERENCES

Abbasi M. and Farbod Y.; 2004: *An introduction to determining the stress status using the reverse method of fault pages and relevant scratches*. Earth Sci., Twelfth Year, 54, 2-9.

Agard P., Omrani J., Jolivet L., Whitechurch H., Vrielynck B., Spakman W., Monié P., Meyer B. and Wortel R.; 2011: *Zagros orogeny: a subduction-dominated process.* Geol. Mag., 148, 692-725, doi: 10.1017/s001675681100046x.

Armijo R., Carey E. and Cisternas A.; 1982: *The inverse problem in microtectonics and the separation of tectonic phases*. Tectonophys., 82, 145-160, doi: 10.1016/0040-1951(82)90092-0.

Central Intelligence Agency; 2007: *Middle East oil and gas.* United States,Washington, D.C., U.S.A., map.

Gartrell A.P. and Lisk M.; 2005: *Potential new method for paleostress estimation by combining 3D fault restoration and fault slip inversion techniques: extraction of fault slip indicators from 3D seismic data. First test on the Skua Field, Timor Sea*. In: Boult P. and Kaldi J. (eds), Evaluating fault and cap rock seals, AAPG Hedberg Series, vol. 2, pp. 23-26.

GCMT (Global Centroid Moment Tensor); 2020: <www.globalcmt.org/home1>.

Gephart J.W. and Forsyth D.W.; 1984: *An improved method for determining the regional stress tensor using earthquake focal mechanism data: application to the San Fernando earthquake sequence*. J. Geophys. Res., 89, 9305-9320, doi: 10.1029/JB089iB11p09305.

Gholami Zadeh P., Adabi M.H., Hisada K., Hosseini-Barzi M., Sadeghi A. and Gassemi M.R.; 2017: *Revised version of the Cenozoic collision along the Zagros Orogen, insight from Cr-spinel and sandstone modal analyses. Geology, Medicine*. Sci. Rep., 7, 10828, doi: 10.1038/s41598-017-11042-1.

IIEES (International Institute of Earthquake Engineering and Seismology); 2006: <www.iiees.ac.ir/en/>.

IRSC (Iranian Seismological Center); 2020: <irsc.ut.ac.ir/>.

Kazem Shiroodi S., Ghafoori M., Faghih A., Ghanadian M., Lashkaripour Gh. and Hafezi Moghadas N.; 2015: *Multi-phase inversion tectonics related to the Hendijan-Nowrooz-Khafji Fault activity, Zagros Mountains, SW Iran*. J. Afr. Earth Sci., 111, 399-408.

Keiding M., Lund B. and Árnadóttir Th.; 2009: *Earthquakes, stress and strain along an oblique plate boundary: the Reykjanes Peninsula, southwest Iceland*. J. Geophys. Res., 114, B09306, doi: 10.1029/2008JB006253.

Kumar A., Singh Sh.K., Mitra S., Priestley K.F. and Dayal Sh.; 2017: *The 2015 April 25 Gorkha Nepal earthquake and its aftershocks: implications for lateral heterogeneity on the Main Himalayan Thrust*. Geophys. J. Int., 208, 992-1008, doi: 10.1093/gji/ggw438.

Lohr T., Krawczyk C.M., Oncken O. and Tanner D.C.; 2008: *Evolution of a fault surface from 3D attributes analysis and displacement measurements.* J. Struct. Geol., 30, 690-700.

Lund B. and Slunga R.; 1999: *Stress tensor inversion using detailed microearthquake information and stability constraints: application to Olfus in southwest Iceland*. J. Geophys. Res., 104B7, 14947-14964.

Lund B. and Bödvarsson R.; 2002: *Correlation of microearthquake body-wave spectral amplitudes.* Bull. Seismol. Soc. Am., 92, 2419-2433.

McKenzie D.P.; 1969: *The relation between fault plane solutions for earthquakes and the directions of the principal stresses*. Bull. Seismol. Soc. Am., 59, 591-601.

MOVE Core (Software); 2009: Petroleum Experts (Petex), Edinburgh, UK, <www.petex.com/products/move-suite/move>.

Pourbeyranvand Sh.; 2012: *Stress changes in Zagros using inversion of focal earthquake mechanisms*. Ph.D. Thesis, Institute of Geophysics, University of Tehran, 147 pp.

Searle M.; 2019: *Geology of the Oman mountains, eastern Arabia*. Springer Nature, Switzerland, 487 pp.

Sepehr M. and Cosgrove J.W.; 2004: *Structural framework of the Zagros Fold-Thrust Belt. Iran.* Mar. Petrol. Geol., 21, 829-843.

Stein S. and Wysession M.; 2003: *An introduction to seismology, earthquakes, and earth structure*. Blackwell Publ., Oxford, UK, 512 pp.

Talebian M. and Jackson J.; 2004: *A reappraisal of earthquake focal mechanisms and active shortening in the Zagros mountains of Iran*. Geophys. J. Int., 156, 506-526.

Tayeb Hosseini F.S., Sepahvand M.R., Abdollahifard I. and Miri S.A.; 2017: *Description of Izeh Hendijan fault using two-dimensional seismic data and seismic data*. Monthly scientific magazine for oil and gas exploration and production, 148, 42-47.

Van Gent H.W., Back S., Urai J.L., Kukla P.A. and Reicherter K.; 2009: *Paleostresses of the Groningen area, the Netherlands - Results of a seismic based structural reconstruction*. Tectonophys., 470, 147-161.

Wessel P., Luis J.F., Uieda L., Scharroo R., Wobbe F., Smith W.H.F. and Tian D.; 2019. *The generic mapping tools version 6.* Geochem., Geophys., Geosyst., 20, 5556-5564, doi: 10.1029/2019GC008515.

World Stress Map; 2020: <www.world-stress-map.org/>.

Corresponding author: Shahrokh Pourbeyranvand
International Institute of Seismology and Earthquake Engineering
No. 21, Arghavan St., North Dibajee, Farmanieh, Tehran, Iran
Phone: +98 21 22831116-9 (ext. 652); e-mail: beyranvand@iiees.ac.ir